THE JOURNAL OF BIOLOGICAL CHEMISTRY
Vol. 279, No. 50, Issue of December 10, pp. 52437–52446, 2004

Printed in U.S.A.

Genome-wide Analysis of Pre-mRNA Splicing

INTRON FEATURES GOVERN THE REQUIREMENT FOR THE SECOND-STEP FACTOR, Prp17 IN *SACCHAROMYCES CEREVISIAE* AND *SCHIZOSACCHAROMYCES POMBE**[S]♦

Received for publication, August 3, 2004
Published, JBC Papers in Press, September 27, 2004, DOI 10.1074/jbc.M408815200

Aparna K. Sapra‡, Yoav Arava§¶, Piyush Khandelia‡, and Usha Vijayraghavan‡‖

From the ‡Department of Microbiology and Cell Biology, Indian Institute of Science, Bangalore 560012, India and the §Department of Biochemistry, Stanford University, Stanford, California 94305-5307

Removal of pre-mRNA introns is an essential step in eukaryotic genome interpretation. The spliceosome, a ribonucleoprotein performs this critical function; however, precise roles for many of its proteins remain unknown. Genome-wide consequences triggered by the loss of a specific factor can elucidate its function in splicing and its impact on other cellular processes. We have employed splicing-sensitive DNA microarrays, with yeast open reading frames and intron sequences, to detect changes in splicing efficiency and global expression. Comparison of expression profiles, for intron-containing transcripts, among mutants of two second-step factors, Prp17 and Prp22, reveals their unique and shared effects on global splicing. This analysis enabled the identification of substrates dependent on Prp17. We find a significant Prp17 role in splicing of introns which are longer than 200nts and note its dispensability when introns have a ≤13-nucleotide spacing between their branch point nucleotide and 3′ splice site. *In vitro* splicing of substrates with varying branch nucleotide to 3′ splice site distances supports the differential Prp17 dependencies inferred from the *in vivo* analysis. Furthermore, we tested the predicted dispensability of Prp17 for splicing short introns in the evolutionarily distant yeast, *Schizosaccharomyces pombe*, where the genome contains predominantly short introns. SpPrp17 was non-essential at all growth temperatures implying that functional evolution of splicing factors is integrated with genome evolution. Together our studies point to a role for budding yeast Prp17 in splicing of subsets of introns and have predictive value for deciphering the functions of splicing factors in gene expression and regulation in other eukaryotes.

Splicing of introns from pre-mRNAs is an essential and ubiquitous process during eukaryotic gene expression. In *Saccharomyces cerevisiae*, ~240 out of the ~6000 ORFs[1] possess introns and only 10 of these genes carry more than one intron. Pre-mRNA splicing, however, is a robust process in this yeast as most of the intron-containing genes are highly expressed (1, 2); thereby, one of every four cellular transcripts requires splicing. The definition of intron-exon junctions, by recognition of the short stretches of conserved sequences in the pre-mRNA, and the two-step transesterification reactions take place in the spliceosome, which is comprised of five small nuclear ribonucleoproteins (snRNPs), U1, U2, U4, U5, and U6, and a large number of proteins. The spliceosomal proteins perform tasks varying from orchestrating the dynamic RNA-RNA interactions to possibly serving as structural scaffolds (3, 4). The functions for most splicing factors have typically been examined on only a select few model pre-mRNAs, like actin and RP51. Therefore, the question of ubiquitous action of splicing factors on all pre-mRNAs, or specialized factors with roles in splicing of subgroups of intron-containing transcripts, remains unanswered at a global scale.

This question is especially pertinent, since some pre-mRNA processing factors are not essential for survival in yeast. Furthermore, over the past decade differential functions for spliceosomal proteins, particularly second-step factors, have been emerging. Among the second-step factors, Prp16, Prp17, Prp18, Slu7, and Prp22, the requirement for the latter three varies with the distance between the branch nucleotide and 3′ splice site in the pre-mRNA (5–7). However, these studies analyzed a small number of transcripts. The applicability of their findings for genome-wide splicing requires testing. A second indicator of functional differences is the influence of some factors on other cellular processes. Prp3/Dbf5, Prp8, Prp17, Prp22, Prp16, and Cef1 have effects on cell cycle progression (8–12). Furthermore, DNA processing and repair defects are seen in alleles of *CLF1/SYF3* and *PRP19* (13, 14). Such overlapping effects could arise from the direct role of a factor in two or more cellular processes or could be a secondary consequence arising from the lack of a spliced mRNA for a gene product functioning in another pathway. These observations highlight the need to examine splicing globally to decipher the dependence of transcripts on a splicing factor and to gain insights on the role of specific spliceosomal proteins.

We have used microarrays, with DNA spots corresponding exclusively to intronic regions in addition to spots for all ORFs, for a global analysis of yeast pre-mRNA splicing. The genome-wide expression profiling was used to identify unique functions for a non-essential splicing factor, Prp17, by comparing the splicing defects among temperature-sensitive *prp17* and *prp22*

* This work was supported in part by an International Senior Research Fellowship from The Wellcome Trust, United Kingdom (to U. V.); by partial infrastructure support from the Indian Council of Medical Research, Government of India; by scholarships (to A. K. S. and P. K.) from Council of Scientific and Industrial Research, Government of India; and by an UNESCO-ASM (2001) short term travel fellowship (to A. K. S.), which facilitated the microarray experiments. The costs of publication of this article were defrayed in part by the payment of page charges. This article must therefore be hereby marked "*advertisement*" in accordance with 18 U.S.C. Section 1734 solely to indicate this fact.

♦ This article was selected as a Paper of the Week.

[S] The on-line version of this article (available at http://www.jbc.org) contains supplemental Figs. 1–3.

¶ Research associate of the Howard Hughes Medical Institute. Present address: Dept. of Biology, Technion, Haifa 32000, Israel.

‖ To whom correspondence should be addressed. Tel.: 91-80-2360-0168; Fax: 91-80-2360-2697; E-mail: uvr@mcbl.iisc.ernet.in or usha_vijayraghavan@yahoo.co.uk.

[1] The abbreviations used are: ORF, open reading frame; nts, nucleotides; WT, wild type.

mutants. We sought to understand whether Prp17 plays a ubiquitous but auxiliary role in splicing of all introns. If not, what are the intron features that predispose a need for Prp17? Based on the shared or unique effects on splicing efficiencies observed in these mutants, we infer a non-ubiquitous role for Prp17. Through an inspection of intron features in all Prp17-dependent substrates, we present evidence for its dispensability when introns have a branch nucleotide to 3′ splice site distance ≤13 nts. Our global analysis also suggests a role for Prp17 in splicing introns longer than 200 nts. We support this prediction by demonstrating the complete non-essentiality of the *Schizosaccharomyces pombe* Prp17 protein, in a genome where the average intron length is only 78 nts. The study thus provides evidence for varying functions of Prp17 in the *S. cerevisiae* genome, allows prediction of its likely substrates in other genomes, and indicates the functions of splicing factors to be integrated with genome evolution.

EXPERIMENTAL PROCEDURES

Strains, Growth Conditions, and Plasmids—Table I lists the strains and plasmids used here. All strains used in the microarray analysis were nearly isogenic to *SS330* and were grown in YPD broth (1% yeast extract, 2% peptone, 2% glucose) at 23 °C to an $A_{600\ nm}$ ~0.6–0.7. Aliquots were withdrawn at time 0 (23 °C) and at 5, 15, 30, 60, and 120 min after shift to 37 °C. Total RNA was extracted by the hot phenol method (15). Actin constructs with a reduced branch nucleotide to 3′ splice site distance were created by loopout PCR on the plasmid SP65-actin (16). The cloned PCR products were termed actin-11pBS and actin-15pBS.

Experimental procedures adopted for *S. pombe* were as described by Moreno *et al*. (17). *spprp17*$^+$ was disrupted in the diploid (MBY102 × MBY103) through homologous replacement with a 2.9-kb *spprp17*Δ::*ura4*$^+$ fragment obtained from the recombinant spprp17Δ pBS. The latter bears a 0.7-kb deletion of the ORF and an insertion of the 1.8-kb HindIII *ura4*$^+$ fragment for selection. The *spprp17*::*ura4*$^+$/*spprp17*$^+$ diploids were verified by Southern blot analysis.

Preparation of Yeast Splicing Extracts and in Vitro Splicing—Splicing extracts from *prp17*Δ *BJ2168* were prepared as detailed by Ansari and Schwer (18). *In vitro* transcription and splicing reactions were according to Vijayraghavan *et al*. (16). WT actin pre-mRNAs were transcribed with SP6 RNA polymerase from the SP65 actin plasmid (16). PvuII restriction fragments from actin-11pBS or actin-15pBS were templates in T7 RNA polymerase transcription reactions. Quantitation of the pre-mRNA, splicing intermediates and products was done by phosphorimaging.

Probe Preparation, Microarray Hybridization, and Data Acquisition—Yeast DNA microarrays were produced and used in hybridizations as described by Derisi *et al*. (19) and Wang *et al*. (20). They contained DNA spots for all the annotated yeast ORFs (as in the *Sacchoromyces* Genome Database) and, in addition, DNA spots for all the predicted introns in genes on the Watson strand (~50% of all introns). There was no bias in these introns with regard to their length, consensus elements, or the gene in which they were present. Intron annotations and distance features were derived from the *Saccharomyces* Genome Database and the MIPS data base (mips.gsf.de/proj/yeast/CYGD). DNA for intron spots was prepared by PCR amplification with a forward primer at the 5′ splice site and a reverse primer at the 3′ splice site. For expression profile analysis, 15 μg of total RNA, from each culture aliquot, was used to generate Cy5-dUTP-labeled cDNA by reverse transcription primed with random 9-mer primers. Sonicated yeast genomic DNA (0.2–0.7 kb) labeled similarly with Cy3-dUTP was the reference probe. Standard protocols for fluorescent labeling, slide processing, hybridization, washing, scanning, and normalization were adopted (cmgm.stanford.edu/pbrown/mguide/index.html).

Northern Blot Analysis of Splicing Defects in S. pombe—Total RNA from *S. pombe* haploid WT *spprp17*$^+$, *spprp17*::*ura4*$^+$, or *prp2-1* cells grown at 23 °C and those transferred to 37 or 18 °C were used for Northern blot analysis as detailed by Urushiyama *et al*. (21).

Reverse Transcription PCR Analysis of S. cerevisiae Transcripts—15 μg of total RNA was the template for first-strand cDNA synthesis with the specified gene-specific exon 2 primer. An aliquot from each reaction was amplified in a 22-cycle PCR by adding the appropriate exon 1 forward primer. These radiolabeled products were resolved on 8% native PAGE gels. Photostimulated luminescence counts for the pre-mRNA and mRNA were obtained in a phosphorimager. These values, normalized to U5 small nuclear RNA levels, were log-transformed to the base 2 and then plotted after zero transformation to the values at 23 °C (0 min time point).

Data Analysis—Microarray data for the time course series of WT, *prp17*Δ, *prp17-1*, and *prp22-1* cells can be obtained from GEO data base (accession number GPL1458). In each time course series, the $\log_2$ (Cy5/Cy3) fluorescence ratios were mathematically "zero-transformed" and analyzed as a function of time relative to the cultures at permissive conditions, *i.e.* time 0 sample. Hierarchical clustering of the data was performed using the program Cluster (22) and visualized in Treeview. A similar clustering of data points is seen when a *k*-means algorithm was employed (data not shown). The data points derived from either of the duplicate experiments were analyzed. After hierarchical clustering, groups of differentially affected intron-containing transcripts were selected by manual inspection. A transcript was considered affected if its expression levels (measured at the ORF spot) decreased, by at least 2-fold and the change persisted (raw data sets available at mcbl.iisc.ernet.in/~pan_sam/prp17.html). In each mutant strain, the intron-containing transcripts were thus classified as affected *versus* unaffected and then subjected to statistical analysis. The primary analysis was an unpaired *t* test and the Mann Whitney test to assess any significant bias between the two groups for the intron features: length, L; the 5′ splice site to branch nucleotide distance, termed A; and the branch nucleotide and the 3′ splice site terminal nucleotide distance (UAC-UAACAN(*X*) PyAG), termed B. A second statistical analysis probed further into this bias by testing several nucleotide lengths, for these intron distance features, as discriminators of the affected or unaffected transcript groups. Significance for each tested cutoff value was determined using a χ^2-test with the degree of freedom being one. The genomic distribution of the number of introns on either side of a chosen cutoff distance served as the expected value. This was compared with the observed value of the number of affected introns, in a mutant, on either side of that specific cutoff.

RESULTS

Increased Precursor and Decreased Message Levels Serve as Global Indicators of Splicing Defects—We have examined the genome-wide effects of splicing factor mutations utilizing DNA microarrays containing all known and predicted *S. cerevisiae* ORFs and spots representing exclusively the predicted intron sequences. To establish the suitability of these arrays as readouts of global splicing defects we studied the consequences of a *ts* mutation in Prp2, an essential helicase required for spliceosome activation prior to catalysis (23). *prp2-1* cells accumulate high levels of pre-mRNAs for several model transcripts. Upon inactivation of *ts prp2-1*, we observe a time-dependent genome-wide increase in the signal intensities at the arrayed intron spots indicating a stable global accumulation of pre-mRNAs (Fig. 1*A*, *filled circles*). Coupled to this is a net decrease in signal intensity at the arrayed ORF spots for intron-containing genes (Fig. 1*A*, *open circles*), despite the fact that the ORF spot can measure both mRNA and pre-mRNA levels. Unlike *prp2-1*, wild type cells held at 37 °C (30 min and longer) show little alteration in either the mRNA or pre-mRNA levels (Fig. 1*B*). These results lead us to infer that for intron-containing transcripts both an increase in signal intensity at the intron spots and the decrease in signal intensity at the ORF spots are quantitative parameters of splicing efficiency.

To establish the role of a new splicing factor, using such arrays, it would be essential to observe an increase in pre-mRNA levels. A decrease in mRNA levels alone, while suggestive of a splicing defect is not conclusive as it may arise from alterations in transcription and/or the decay rate of the mRNAs. However, quantitation of the mRNA species is a more suitable index for comparison of known splicing mutants, since altered mRNA levels cause cellular phenotypes. Furthermore, the data from intron spots alone are inadequate for comparison between mutants, since the levels of accumulated intermediates and pre-mRNAs vary (Ref. 24 and this study). We have therefore used the ORF spot measurements, which reflect largely the spliced mRNA levels (see following section), to compare expression profiles among and within splicing mutants.

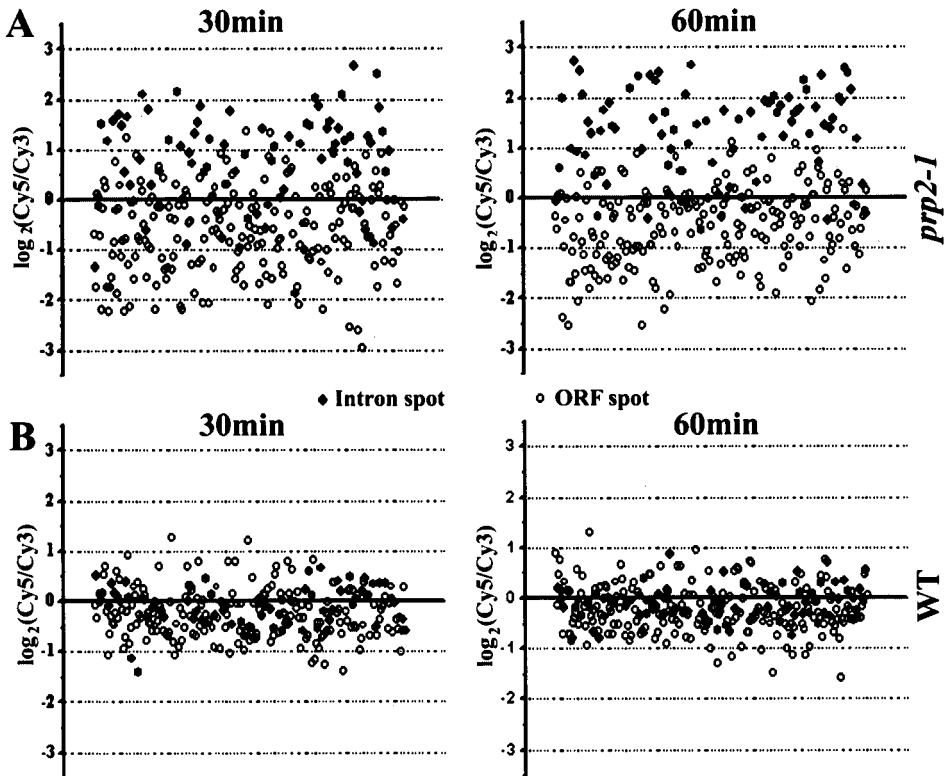

FIG. 1. **Global increase in pre-mRNA and decrease in mRNA levels indicate splicing defects.** *A*, scatter plot of the signal intensity ($\log_2$ Cy5/Cy3), for intron-containing transcripts, detected at the intron spots (●) and their corresponding ORF spots (○), 30 and 60 min after inactivation of *ts prp2-1*. The *x*-axis plots these transcripts arranged alphabetically from *left* to *right*. *B*, ratios of signal intensities in identically treated wild type cells: ● shows intron spot data and ○ the ORF spot data.

The data from the intron spot was taken into account where relevant and available.

Global Analysis of Splicing in Two Second-step Factors and Their Differential Requirements—We next analyzed splicing derangements in *ts* alleles of two second-step factors, Prp17 and Prp22 (Table I) (7, 25, 26), using temperature-shift protocols similar to that used for *prp2-1*. The global effect on the ratio of precursors to message (p/m) in *prp17*Δ, *prp17-1*, and *prp22-1* cells indicates splicing defects to set in between 15 and 30 min of temperature shift (supplemental Figs. 1 and 2). In these mutants, a clustering of the expression level changes for intron-containing transcripts, as detected at the arrayed intron and ORF spots, reveals two prominent clusters. They comprise the most severely and the most similarly affected transcripts in these mutants (Fig. 2*A*, *red* and *green bars*). The *red bars* represent a majority of the intron spots where the build-up of splicing intermediates and precursor RNAs is sensed as increased signal intensity at the arrayed intron spots. This profile is most evident in *prp22-1* and does not occur in wild type cells. The second cluster, marked by the *green bar*, represents expression profiles for a subset of the arrayed ORF spots representing intron-containing transcripts encoding ribosomal proteins. The immediate heat shock response of reduced transcription from these genes (27) occurs in both the wild type and mutant cells (Fig. 2*A*, *green bar*). In wild type cells, the transcript levels recover from this effect (Fig. 2*A*, *green bar*, compare *lanes 2–4* in WT), but the mutants differ in their persistently reduced signal intensities for these intron-containing transcripts.

Besides these two easily identified clusters, we observe clustered data points for several other transcript groups that differ in their severity of expression changes or in their response among various strains (Fig. 2*A*, *black bars* to the *right*). Several of these differentially affected clusters of transcripts are shown in Fig. 2, *B–G*. They can be classified as those affected similarly in all the mutant strains (Fig. 2, *D* and *F*), those affected maximally in *prp22-1* (Fig. 2*B*), those with a persistent reduction in the *prp17* alleles (Fig. 2, *C* and *E*), and those most affected in *prp17*Δ (Fig. 2*G*). Global analysis of splicing defects through these microarrays, therefore, reaffirms the existence of differential *in vivo* splicing factor requirements and aids in categorization and analysis of groups of transcripts with shared or unique dependence on specific factors.

ORF Spots Measure mRNA Levels; Microarray Results Validated through Reverse Transcription PCR Analysis—The arrayed ORF spots contain the entire ORF sequence and therefore can hybridize with both the mRNA as well its precursor RNAs. Thus, the decrease in mRNA levels in a splicing mutant may mask the increase in unspliced precursors. However, the microarray data reveal a temporal decrease in intensity measured at the ORF spot (exemplified in Fig. 2*A*, *green bar*). This occurs reproducibly even in the *prp2-1* (Fig. 1*A*, *unfilled circles*) and *prp22-1* mutants (Fig. 2*A*, *lanes 2–6*) that accumulate pre-mRNAs. To decipher the correlation between the data from an ORF spot and the individual pre-mRNA and mRNA levels, we used semiquantitative reverse transcription PCR to independently assess the precursor (P) and mRNA (M) levels in these mutants. Fig. 3, *A–C*, present the data for three representative intron-containing transcripts. The fold changes in normalized mRNA levels (Fig. 3, *gray bars*) and the combined precursor and mRNA levels (Fig. 3, *white bars*) are plotted with reference to the levels at permissive conditions (0 min). These data, for the cultures 30 and 60 min after temperature-shift, were compared with fold changes as detected at the ORF spot from microarray data (Fig. 3, *black bars*). We find the intensities at the microarray ORF spots (*black bars*) to correlate better with the mRNA levels (*gray bars*) rather than to the combined mRNA and pre-mRNA levels (*white bars*). This is particularly

TABLE I
Strains and plasmids used in the study

Strain	Genotype	Reference
SS330B (WT)	*MAT a ade2–101 his3Δ200 ura3–52 tyr1 suc2 bar1::hisG*	This study
prp17Δ	*prp17Δ::HIS3 MAT a ade2–101 his3Δ200 ura3–52 tyr1 suc2 bar1::hisG*	This study
prp17-1	*prp17-1 MAT a ade2–101 his3Δ200 ura3–52 tyr1 suc2 bar1::hisG*	This study
prp2-1	*prp2-1, MAT a ade2–101 his3Δ200 ura3–52 tyr1 suc2 bar1::hisG*	This study
prp22-1	*prp22-1 MAT a ade2–101 his3Δ200 ura3–52*	Vijayraghavan *et al.* (15)
prp17ΔBJ	*MAT a prp17::LEU2 ura3–52 trp1 leu2–3 leu2–112*	Jones *et al.* (25)
MBY102	h^+ *ade6–210 leu1–32 ura4-D18*	Dr. M. Balasubramanian
MBY103	h^- *ade6–216 leu1–32 ura4-D18*	Dr. M. Balasubramanian
spprp17Δ	*h, spprp17::ura4*$^+$ *ade6 leu1–32 ura4-D18*	This study
spprp2-1	h^- *prp2-1 leu2-1*	Dr. K. Gould
Actin-11 pBS	Actin minigene with intron branch nucleotide to 3′ splice site distance of 11 nts	This study
Actin-15 pBS	Actin minigene with intron branch nucleotide to 3′ splice site distance of 15 nts	This study
spprp17Δ pBS	*spprp17*$^+$ clone with ORF deletion and disruption with *ura4*$^+$ cassette	This study
SptfIId-E3pBS	A 0.34-kb sptfIId$^+$ cDNA fragment cloned in pBS-KS	This study

the case for mutants like *prp17* where only marginal accumulation of pre-mRNA occurs, making the change in (P + M) nearly equal to the change in M. Notably, even in *prp22-1* a net decrease in signal intensity at the microarray ORF spot is detected (Fig. 2*A*, *prp22-1,* cluster marked with the *green bar*). In agreement with this observation, the reverse transcription PCR analysis also indicates the data from the ORF spot to largely correlate with the relative changes in mRNA levels (Fig. 3*A–C*, compare the *black* and *gray bars* in *prp22-1*). This is perhaps due to the significant difference in the relative cellular abundance of these two RNA species, pre-mRNA and mRNA. The pre-mRNA levels are normally very low and in a splicing factor mutant, despite the severalfold increase their absolute amounts may remain far lower than that of mRNA, therefore causing a minimal effect on the signal intensities at the ORF spots.

Intron Features Govern the Requirement for Prp17—Common features in some subgroups of intron-containing transcripts could predispose them to greater or lesser extent on a specific factor. To identify any such features correlating with dependence on Prp17, all the intron-containing transcripts affected in *prp17*Δ cells were compared with the data from *prp22-1*. ORF spots for the 242 intron-containing transcripts reveal 132 affected transcripts in *prp17*Δ (Fig. 4*B*, *checkered circle*; also see supplemental Fig. 3 for list), while a partially overlapping set of 110 transcripts are affected in *prp22-1* (Fig. 4*B*, *gray circle;* see supplemental Fig. 3 for list). The splice site and branch point consensus elements showed no consistent deviations that can explain the dependence on or independence from Prp17. We then analyzed the following parameters: the intron length (L), spacing between the 5′ splice site and the branch nucleotide (A), and the spacing between the branch nucleotide and the 3′ splice site (B) (Fig. 4*A*). For each feature, we examined any bias in the distribution of intron-containing transcripts that are affected in *prp17* or *prp22* mutants (Fig. 4, *C–H*, *black bars*) in comparison with the genomic distribution (Fig. 4, *C–H*, *white bars*). While Prp17 and Prp22 influence the splicing of a few short introns, they are both distinctly required for splicing most introns longer than 200nts (Fig. 4, *C* and *D*, *black bars*). χ^2 values were determined for distribution, of affected *versus* unaffected transcripts, on either side of several empirically chosen nucleotide lengths. In the case of total intron length, a cutoff of 200 nts distinguishes the affected class of transcripts with statistically validated significance ($\chi^2 = 1.8 \times 10^{-6}$ for Prp17 and 0.001 for Prp22). These observations indicate a global Prp17 requirement for splicing introns longer than 200 nts.

As a corollary to the above prediction, we find that an increased distance between the 5′ splice site and branch nucleotide is a parameter shared by Prp17- and Prp22-dependent transcripts (Fig. 4, *E* and *F*, *black bars*). Here too a spacing of A = 200 nts is statistically validated as a discriminating feature between the dependent and independent classes of transcripts. The distance between branch nucleotide to 3′ splice site (B) varies unimodaly in the genome (Fig. 4, *G* and *H*, *white bars*). Distribution of Prp17 and Prp22 dependent transcripts for this feature also follows this pattern (Fig. 4, *G* and *H*, *black bars*). Earlier *in vitro* studies, with modified actin transcripts, have shown Prp22 independent splicing when the branch nucleotide to 3′ splice site distance was less than 26 nts (7). However, our genome-wide data indicate a significant global Prp22 independence only when this intron parameter is 15 nts ($\chi^2 = 0.02$) or lower (Fig. 4*H*, B = 13; $\chi^2 = 0.017$). Dispensability of Prp17 is a property shared by substrates with the branch nucleotide to 3′ splice site distance of 13 nts or lower ($\chi^2 = 0.008$, Fig. 4*G*). This correlation for a genome-wide independence from Prp17 is not very significant ($\chi^2 = 0.06$) for transcripts with a distance of 15nts or lower. In summary, the microarray data reveal a great majority of introns with length >200 nts to depend on Prp17. The data also indicate a dispensability of Prp17 when introns have a short branch nucleotide to 3′ splice site distance (*i.e.* B ≤ 13 nts). We additionally define the global requirement for the second step functions of Prp22 to those introns with a branch nucleotide to 3′ splice site distance ≥15 nts.

Prp17 Is Dispensable for the Splicing of Introns with a Branch Nucleotide to 3′ Splice Site Distance ≤13 nts—None of the above intron parameters can alone explain the requirement for Prp17. We therefore analyzed a combination of these features, *i.e.* a ratio of the 5′ splice site to branch nucleotide distance to the spacing between the branch nucleotide and the 3′ splice site (A/B). To study the covariance of the two features, we plotted the values of B against A/B and compared the affected *versus* unaffected transcript sets in *prp17*Δ (Fig. 5*A*, *unfilled* and *filled circles*, respectively). We discern that splicing of several, but not all introns, with very low A/B ratios (≤2) are unaffected by the absence of Prp17 (Fig. 5*A*, below demarcating *horizontal line*). Importantly, in concordance with the χ^2 value of 0.008 (Fig. 4*G*), we observe that substrates with B values ≤13 nts are unaffected in *prp17*Δ irrespective of the distance parameter A (Fig. 5*A*, *left* of demarcating *vertical line*). The microarray data thus predict a precise branch nucleotide to 3′ splice site distance in Prp17 independent substrates.

This predicted dispensability of Prp17 for splicing of subsets of the global pre-mRNAs was tested *in vitro*. Modified actin transcripts with varying branch nucleotide to 3′ splice site distances were tested in extracts from *prp17*Δ cells grown at 23 °C. We compared *in vitro* splicing of actin transcripts with

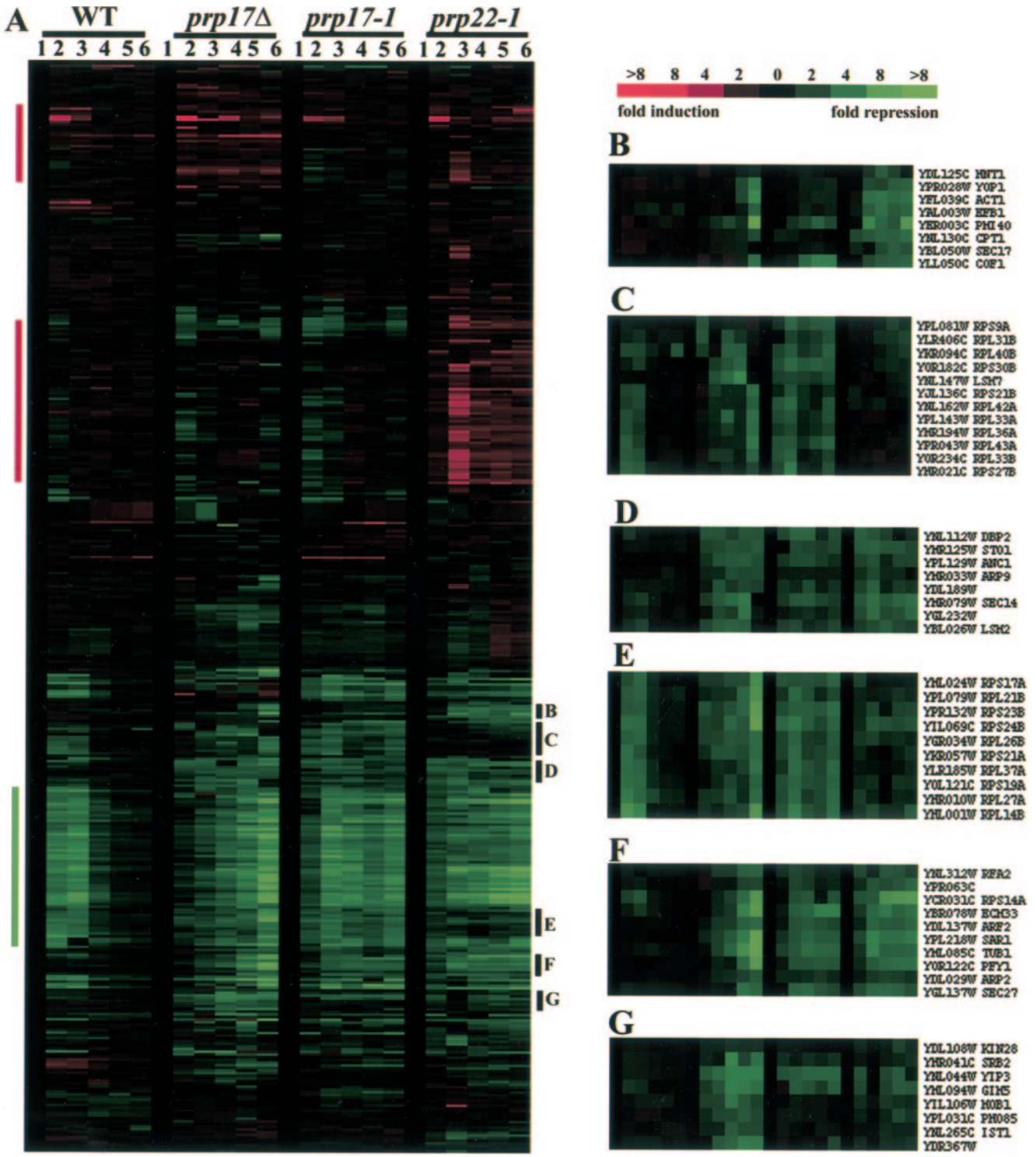

FIG. 2. **Global view of splicing defects in *prp17* and *prp22* mutants.** *A*, hierarchical clustering of intron-containing transcripts showing fold induction or repression in their expression levels as detected at 242 ORF spots and 167 of the corresponding intron spots. Changes in expression levels 5, 15, 30, 60, and 120 min (*lanes 2–6*) after shift to 37 °C are shown relative to the 0 min time point (*lane 1*). The *green vertical bar* to the *left* highlights a cluster with severely decreased expression sensed at the ORF spots. The *red vertical bars* highlight the response of several transcripts with increased signal intensity at their intron spots. The *gray color* represents spots that could not be scored, in one or more of the time points, of the experiment shown. Rows of data points outside the highlighted *red* and *green bars* are largely ORF spots with a few intron spots. The scale bar for the intensity changes is shown to the *right*. *B–G*, clusters of intron-containing transcripts with differential splicing defects. *B*, transcripts were affected most in *prp22-1*. *C* and *E*, transcripts with compromised splicing in the *prp17* alleles. *D* and *F*, transcripts affected similarly in all the mutant strains. *G*, transcripts with the strongest expression level decrease in *prp17*Δ cells. This cluster can be viewed at mcbl.iisc.ernet.in/~pan_sam/prp17.html.

the wild type branch nucleotide to 3′ splice site distance (43 nts) to that of a substrate with a 15nts spacing (higher than the predicted value for Prp17 dispensability) and another with a 11 nts spacing (lower than the predicted value of 13 nts for Prp17 dispensability). The *in vitro* reactions were performed at the permissive temperature, 23 °C, and at the non-permissive temperature of 37 °C, where Prp17 is essential for viability and for the second step of splicing (15, 25, 26). The actin-43 transcript,

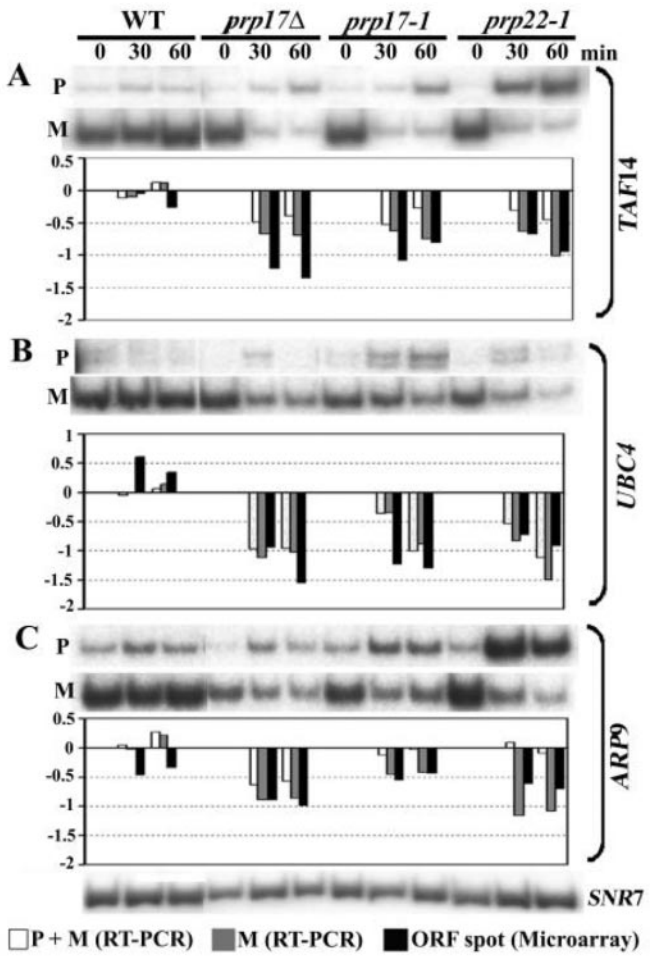

FIG. 3. **Reverse transcription PCR analysis of three intron-containing transcripts; comparisons with the microarray data.** Exon 2 primers for *A*, *TAF14*/*ANC1*, *B*, *UBC4*, and *C*, *ARP9* were used for reverse transcription followed by limiting PCR in combination with the appropriate exon 1 primer. Quantitation of the resolved PCR products determined each of the pre-mRNA (*P*) and mRNA (*M*) levels. These values normalized to *SNR7* levels, an intronless transcript, are log-transformed to base 2 and plotted on the *y*-axis. *Bars* represent the fold change, relative to the 0-min time point, occurring 30 or 60 min after temperature shift. In all cases, the *gray bars* show the mRNA levels, the *white bars* the combined mRNA and pre-mRNA levels, and the *black bars* the data from the ORF spot of the microarray experiments.

with wild type spacing between the branch nucleotide and 3′ splice site, was completely and efficiently spliced at 23 °C (Fig. 5*B*, *lanes 1–3*) and the second-step products accumulate (Fig. 5*E*, *black bars* in *columns 1–3*). There was no kinetic lag for the second-step at this temperature. In contrast, the second step of splicing is nearly arrested in reactions carried out at 37 °C (Fig. 5*B*, *lanes 4–6*) leading to an accumulation of splicing intermediates generated by the first-step reaction (Fig. 5*E*, *white bars* in *columns 4–6*). These data conform to previous *in vitro* reports and explain the lethality of *prp17*Δ cells at 37 °C (15, 25, 26). The actin-15 substrate shows marginally decreased kinetics for the second-step at 23 °C (Fig. 5*C*, *lanes 1–3*; compare *black bars* in *columns 1–3* of Fig. 5*F* with Fig. 5*E*). This effect is greatly exacerbated in reactions done at 37 °C (Fig. 5*C*, *lanes 4–6*; Fig. 5*F*, compare *black bars* in *columns 4–6* with *columns 1–3*), indicating a role for Prp17 for the second-step splicing of introns with a B distance of 15 nts. Strikingly, in the absence of Prp17, the actin-11 transcript is efficiently spliced (Fig. 5*D*) at both temperatures (Fig. 5*G*, compare *black bars* in *columns 1–3* with *columns 4–6*). Thus, a decrease of 4 nts in the branch nucleotide to 3′ splice site distance confers independence from Prp17. These *in vitro* experiments thus corroborate our prediction of 13 nts between the branch nucleotide and the 3′ splice site as a distinguishing feature for independence from Prp17.

S. pombe Genome Expression, with Predominantly Small Introns, Does Not Require Prp17—PRP17 is evolutionarily conserved, and its homologues are computationally identified in *Homo sapiens*, *Caenorhabditis elegans* and the fission yeast *S. pombe* (28, 29). Our genome-wide analysis in *S. cerevisiae* predicts a greater Prp17 role in splicing of long introns (>200 nts). To examine the validity of this prediction for other genomes where introns are prevalent in most genes, we have assayed the role of the *S. pombe PRP17*. This evolutionarily distant yeast possesses ~4730 pre-mRNA introns with multiple introns per gene. Interestingly and unlike *S. cerevisiae* a majority of the fission yeast introns are short, *i.e.* 40–80 nts; only ~6% are longer than 200 nts (Fig. 6*A*). If Prp17 functions are critical for the splicing of long introns then the phenotypic consequences of its absence in *S. pombe* may be less severe than that in budding yeast.

We have created a null allele for the genomic *spprp17*$^+$ locus in the diploid *spprp17*::*ura4*$^+$/*spprp17*$^+$. This diploid was sporulated and tetrads dissected (Fig. 6*B*). In all tetrads we obtained four viable spores at 23 °C, two of which carried the null allele (ura$^+$), the other two being wild type (ura$^-$). We infer that the *spprp17*Δ cells are viable. Thus like in *S. cerevisiae*, the *S. pombe PRP17* function is non-essential at 23 °C. However, unlike in *S. cerevisiae*, the fission yeast null mutant does not display any conditional phenotype. Its growth rates are comparable with the wild type at all the temperatures tested (Fig. 6*C*). The effect on pre-mRNA splicing, in *spprp17*Δ cells, was assayed by determining the splicing status of the intron-containing *sptfIId*$^+$ transcripts. No decrease in mRNA levels are seen at any of the growth temperatures in cells lacking Prp17 (Fig. 6*D*, *arrow M*, *lanes 4–6* and *lanes 9–11*). Furthermore, no accumulation of unspliced precursors occurred at either 18 or 37 °C (Fig. 6*D*, *arrow P*, *lanes 4–6* and *lanes 9–11*). This contrasts with the compromised mRNA levels and moderate accumulation of pre-mRNA in *S. cerevisiae prp17*Δ cells grown even at the permissive temperature (15, 30), a condition exacerbated at higher temperatures. Together, these data point to the dispensability of Prp17 in a genome with predominantly small pre-mRNA introns.

DISCUSSION

DNA microarrays to analyze genome-wide functions of splicing factors and their effects on gene expression offer great potential to study post-transcriptional regulation. Parallels can be made between such analysis with spliceosomal factors and studies on the RNA polymerase II transcriptional machinery (2, 31, 32). Both these macromolecular complexes execute and modulate genome interpretation. Genome-wide functional analyses of splicing factors are as yet uncommon with only a single global analysis of yeast splicing factors (24). This study utilized oligonucleotide arrays to detect the splicing status of intron-containing transcripts alone. Few other reports have demonstrated microarray or fiber-optic arrays to work in principle for global analysis of alternative splicing in human cells (33, 34).

We report here microarray analysis of pre-mRNA splicing mutants of *S. cerevisiae* with special focus on the second-step factor Prp17. By analyzing two *ts* mutants, *prp17* and *prp22*, we have established the facile use of microarrays with intron spots and ORF spots for global analysis of splicing. In these microarrays the ORF spots report global splicing defects by detecting quantitative reductions in spliced mRNA levels. This can be further coupled to the quantitative detection of the accumulated splicing intermediates or precursor RNAs using

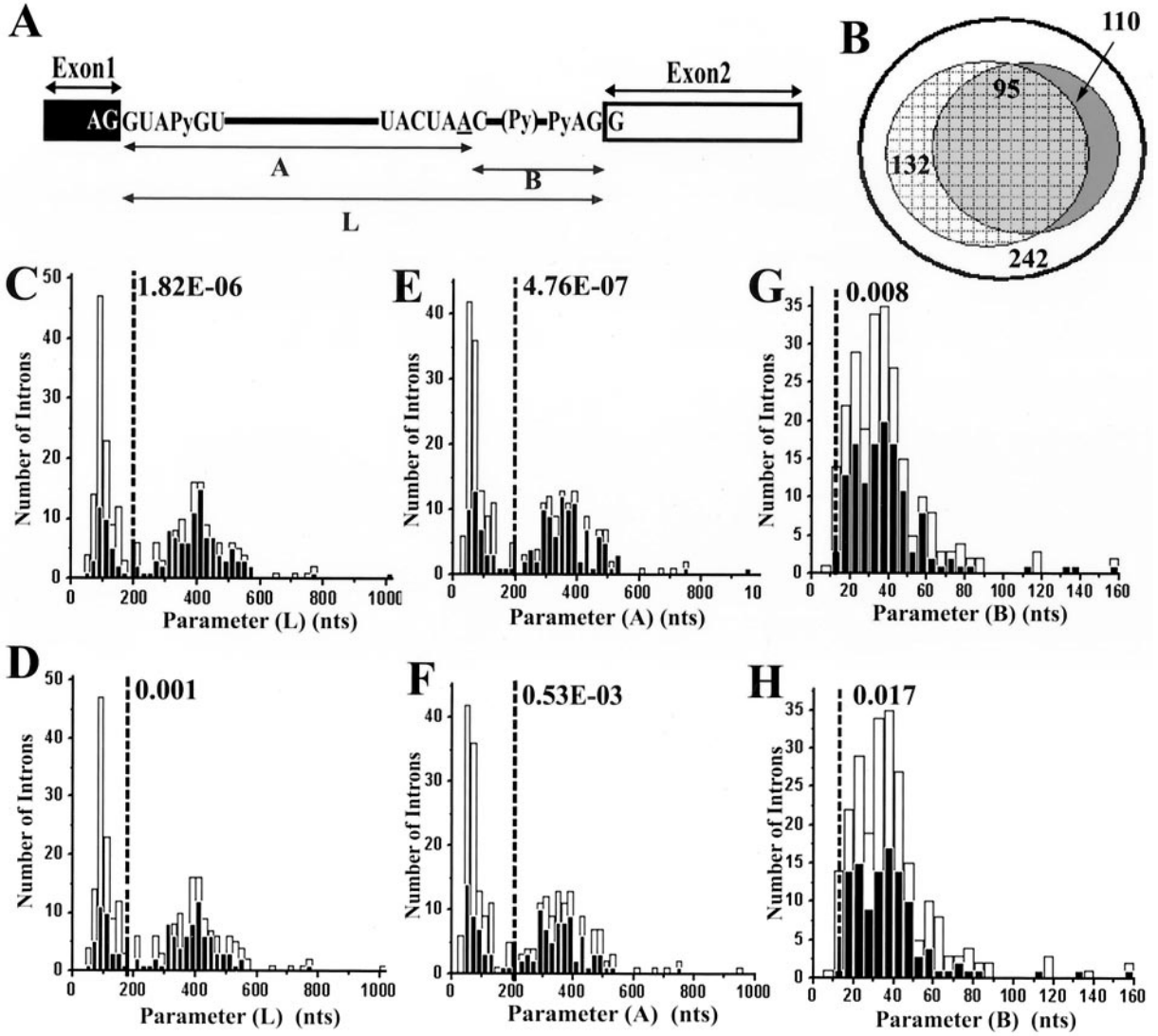

FIG. 4. **Intron features and predisposition for splicing factors**. *A*, schematic representation of conserved intron sequences and their relative spacing. *B*, Venn diagram depicting the common and unique sets of affected transcripts in *prp17*Δ (*checkered*) and *prp22-1* (gray), among the 242 intron-containing transcripts analyzed by their ORF spot data. *C–H*, Graphs analyzing three intron length parameters and their relationship to Prp17 or Prp22 dependence. In each graph, the number of introns (*y*-axis) is plotted against length, in nts (*x*-axis), for that feature. *C* and *D*, distribution of intron lengths, L, in the genome is indicated by *white bars*. The *black bars* indicate Prp17 (*C*)- and Prp22 (*D*)-dependent transcripts. χ^2 values, for factor dependence in introns >200 nts, are marked along the *dashed vertical line*. *E* and *F*, distribution of 5′ splice site to branch point nucleotide distance, A, in all predicted introns shown as *white bars*. The *black bars* are the Prp17 (*E*)- and Prp22 (*F*)-dependent transcripts. χ^2 values, for the factor dependence in the subgroup with A >200 nts, is shown along the *dashed vertical line*. *G* and *H*, genomic variation for the branch nucleotide to 3′ splice site distance, B, marked in *white bars*. The Prp17 (*G*)- or Prp22 (*H*)-dependent subsets are shown as *black bars*. Introns with B ≤13 nts are independent of these factors (χ^2 = 0.008 for Prp17 and 0.017 for Prp22).

the data from the arrayed intron spots. Our general inferences compare with the earlier report of Clark *et al.* (24) where splice-junction oligonucleotides together with intron-specific probes detected global splicing defects. Both studies do not find a significant accumulation of precursor RNAs in *prp17*Δ. This contrasts with the stable high levels of unspliced RNAs seen in *prp2* and *prp22* (this study) and *prp4* (24). The data indicate the operation of multiple alternate pathways for precursor RNA degradation, perhaps arising from the varied stability of the arrested spliceosomes. We find a significant global decrease in mRNA levels for intron-containing transcripts, in *prp17*Δ cells, a phenotype reported as lower splice-junction indexes by Clark *et al.* (24). Our temporal analysis reveals that this effect is rapid and detectable, for certain transcripts, within 15 min of transfer to non-permissive conditions (Fig. 2 and supplemental Fig. 2).

Varied dependencies of splicing substrates on factors have previously been suggested from *in vitro* analyses with model transcripts (5–7). A Prp17 role was recently shown for the splicing of the *ANC1* intron where the nucleotides flanking the branch point consensus sequence and those upstream of the 3′ splice site were defined as contributory cis-elements (35). Removal of this intron could partially relieve the cell cycle phenotypes of *prp17*Δ cells but not its temperature-sensitive lethality. Our global analyses also detect severe reduction in *ANC1* mRNAs (Fig. 3*A*). Deciphering the precise global role of a factor can be aided by a genome-wide analysis of its likely substrates. We infer a greater dependence on Prp17 when introns are longer than 200 nts. By testing this observation on the *S. pombe* genome with predominantly small introns, we validate the predictive nature of the global analysis in *S. cerevisiae*. The lack of any significant growth phenotype in fission *spprp17*Δ cells points to the complete dispensability of this factor in genomes with small introns. The few introns (~6%) in *S. pombe* that are longer than 200 nts may have other features conferring independence from Prp17, such as a favorable

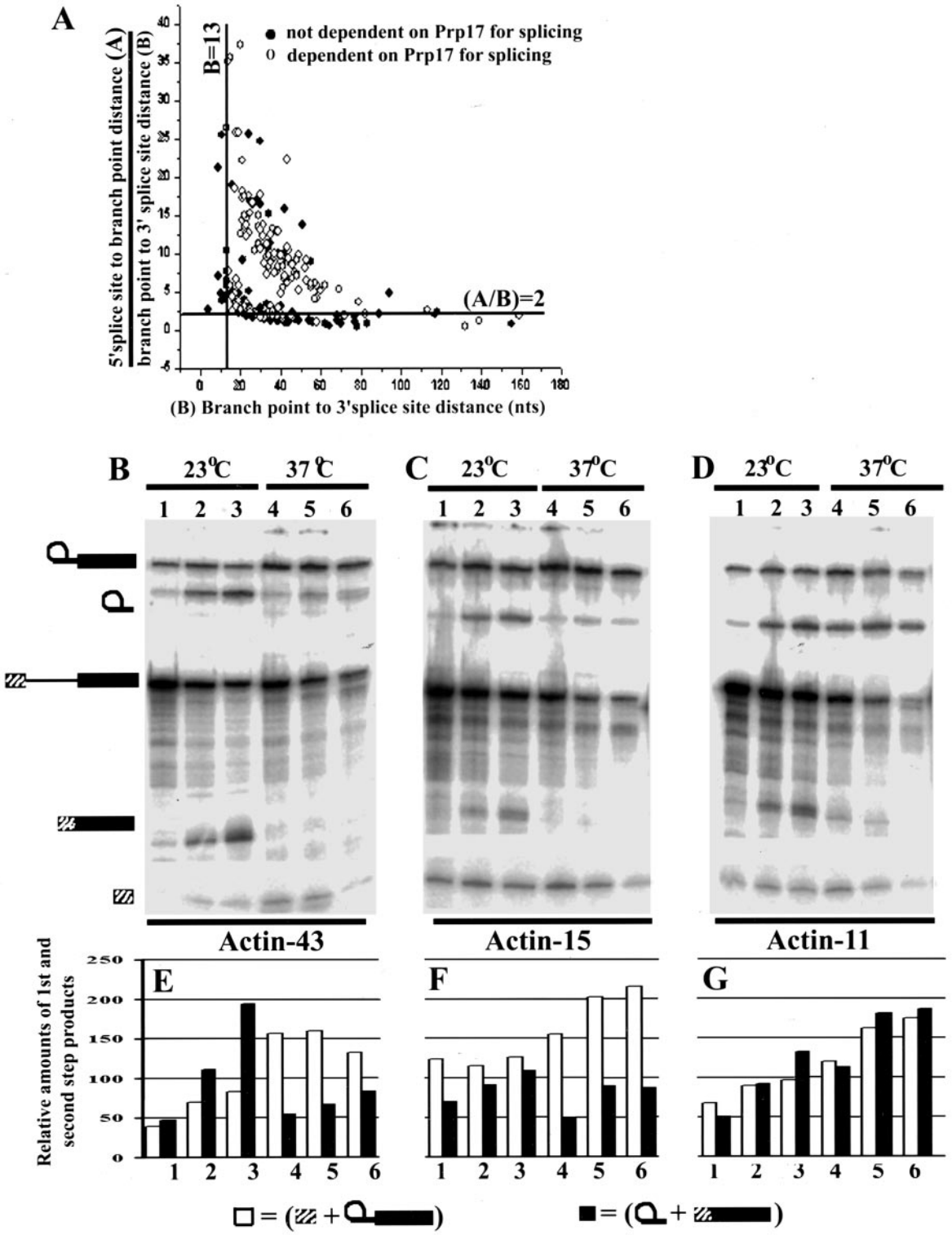

FIG. 5. **Prp17 is dispensable for splicing of introns with B distance ≤13.** *A*, scatter plot of the parameter B (*x*-axis) *versus* the A/B ratio (*y*-axis) for *prp17*Δ unaffected (*filled circles*) and *prp17*Δ affected (*open circles*) intron-containing transcripts. The *vertical line* marks a B distance of 13 nts. The *horizontal line* marks an A/B ratio of 2. *B–D*, *in vitro* splicing of wild type or modified actin substrates, with *prp17*Δ extracts, at 23 or 37 °C as indicated above the lanes. Aliquots withdrawn at 5, 15, and 30 min (*lanes 1–3* or *4–6*) for each of the substrates, actin-43 (*panel B*), actin-15 (*panel C*), and actin-11 (*panel D*), were resolved. The substrate pre-mRNA, the first- and second-step reaction products, are diagrammatically represented. *E–G*, assessment of the first- and second-step reaction efficiencies for data panels *B–D*. First- and second-step products in each lane were quantitated and normalized with respect to the pre-mRNA. The relative amounts of first (*white bar*) and second (*black bar*) step products for each lane (*1–6*) are plotted.

branch nucleotide to 3′ splice site spacing. Alternatively, *S. pombe* transcripts with long introns may encode proteins non-essential for survival. Importantly, these preliminary data demonstrate that functions for splicing factors are integrated with genome evolution. When applied to other organisms these inferences may provide clues to investigate regulation of splicing in the context of development and disease.

Our global analysis indicate the splicing of budding yeast

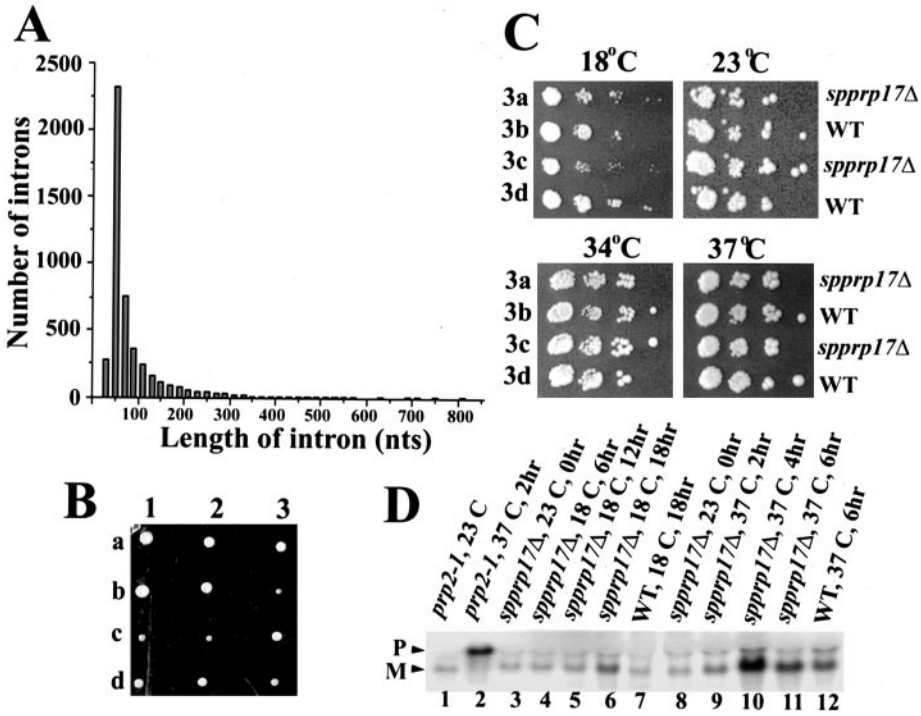

FIG. 6. **Prp17 is dispensable for the *S. pombe* genome.** *A*, frequency distribution of introns in the fission yeast genome. Most introns are 40–60 nts long. *B*, complete spore viability (*a–d*) for three representative tetrads (*1–3*) from the diploid *spprp17*::*ura4*$^+$/*spprp17*$^+$ are shown. *C*, the *spprp17*::*ura4*$^+$ null allele does not confer growth phenotypes at 18, 23, 34, or 37 °C. Serially diluted cells from the four spores of a tetrad (*3*) tested for growth rate differences. *D*, Northern blot analysis of splicing efficiency in *spprp17*::*ura4*$^+$, *prp2-1*, and wild type cells. Pre-mRNA (*P*) and mRNA levels (*M*) were assessed for the intron-containing transcript, *sptfIId*$^+$, in cells grown at 23 °C (*lane 3* and *8*) compared with those transferred to 18 °C for 6, 12, and 18 h (*lanes 4–6*) or those transferred to 37 °C for 2, 4, and 6 h (*lanes 9–11*). Similarly treated isogenic wild type cells (18 °C, *lane 7* and 37 °C, *lane 12*) served as controls. *ts prp2-1* (*lanes 1–2*), which accumulates unspliced precursors, was the positive control.

introns with a branch nucleotide to 3′ splice site distance ≤13 nts to occur independent of Prp17. *In vitro* experiments support this finding and taken together demonstrate a Prp17 role for splicing certain subsets of cellular transcripts. The general conclusions drawn by Clark *et al.* (24) were similar but did not define criteria for Prp17 dependence. They report some transcripts with relatively short branch nucleotide to 3′ splice site distance to be unaffected by the loss of Prp17. We surmise the same and find that by defining a maximum distance of 13 nts we can distinguish Prp17 independent substrates. A similar spacing, *i.e.* >12 nts, is proposed to impose a need for Slu7, an essential second-step factor (6). This would exclude seven intron-containing transcripts, in the yeast genome, from dependence on Slu7. For Prp17 our data implicates 12 pre-mRNAs, in the genome, to be independent of Prp17.

Of the six factors, Prp16, Prp17, Prp18, Slu7, Prp8, and Prp22, contributing to 3′ splice site selection during the second step of splicing, Prp18, Slu7, and Prp22 are dispensable when substrates have short branch nucleotide to 3′ splice site distances (5–7). In the second step, Prp17 acts at or about the time of the Prp16-dependent spliceosome remodelling (25). Interestingly, *in vitro* splicing of modified actin substrates with altered branch nucleotide to 3′ splice site distances required Prp16 function ubiquitously (5), implicating this conformational rearrangement to be essential for all substrates. Prp17 perhaps plays a context-dependent function. Prp17 is needed for the strong cross-linking of Prp8 and Slu7 with the 3′ splice site (36). Interactions between Prp8, Slu7, and Prp17 are supported by both cross-linking and genetic interaction studies (36–38). Perhaps in pre-mRNAs with a short branch nucleotide to 3′ splice site distance the alignment of the 3′ splice site to the active site occurs in the absence of Prp17 or Slu7, allowing such introns to be processed by the two essential factors, Prp16 and Prp8.

While many introns with long branch nucleotide to 3′ splice site distances are Prp17-dependent (Fig. 4*G*) this parameter does not always apply. In fact, an early investigation on actin pre-mRNA showed critical spacing requirements between the 5′ splice site and branch point (A) and between the branch point and 3′ splice site (B) to operate for efficient splicing (39). A greatly shortened intron (L = 73 nts; B = 43; A/B = 0.7), with reduced spacing between the 5′ splice site and the branch point, was not spliced (39). Increasing the overall intron length, by increasing the 5′ splice site and branch point distance (L = 87 nts; B = 43; A/B = 1), or reducing the spacing between the branch point and 3′ splice site (L = 73 nts; B = 29; A/B = 1.5) could alleviate the defect. These results indicate the spacing between intron recognition elements to influence splicing independent of the intron length. We studied the combined effects of the 5′ splice site to branch nucleotide distance and the branch nucleotide to 3′ splice site distance by examining their ratio (A/B) in Prp17-dependent and -independent substrates. Our microarray data show nearly all introns with an A/B ratio <2 to be Prp17-independent regardless of the distance between their branch nucleotide and 3′ splice site (*i.e.* B). Mechanistically one can envisage a role for Prp17 in facilitating interactions between the two splice sites. Evidence supporting this speculation are first, *prp17* mutants in addition to an arrested second step are marginally compromised for the first-step of splicing (25, 26). Second, Prp17 is a component of the Cef1p complex (40, 41) and displays genetic interaction with many of its factors including *CLF1*/*SYF3* (42). Interestingly, Clf1p associates with both the U1 and U2 snRNPs in early prespliceosomes (43). Third, Prp17 itself is present in early pre-catalytic

spliceosomes.[2] These findings together suggest a role for Prp17, along with other components of the Cef1 complex, in maintaining bridging interactions across the length of the intron.

Pre-mRNA splicing operates not only to prepare a functional transcript or its differentially spliced forms for translation but can be critical for regulation of several cellular processes. Global analysis of splicing in simple eukaryotes, like yeast, have predictive value in understanding the role of splicing factors in the interpretation of complex genomes.

Acknowledgments—We thank Profs. D. Herschlag and P. O. Brown, Stanford University, for their interest and resources for microarray experiments. We also thank all members of the Herschlag and Brown laboratories. The design of the intron arrays by Dr. V. Iyer is acknowledged. We thank Profs. N. V. Joshi, of CES, and R. Hariharan, of CSA, Indian Institute of Science, for guidance in statistical analysis and software.

REFERENCES

1. Spingola, M., Grate, L., Haussler, D., and Ares, M. Jr. (1999) *RNA* (*N. Y.*) **5,** 221–234
2. Holstege, F. C., Jennings, E. G., Wyrick, J. J., Lee, T. I., Hengartner, C. J., Green, M. R., Golub, T. R., Lander, E. S., and Young, R. A. (1998) *Cell* **95,** 717–728
3. Brow, D. A. (2002) *Annu. Rev. Genet.* **36,** 333–360
4. Jurica, M. S., and Moore, M. J. (2003) *Mol. Cell* **12,** 5–14
5. Brys, A., and Schwer, B. (1996) *RNA* (*N.Y.*) **2,** 707–717
6. Zhang, X., and Schwer, B. (1997) *Nucleic Acids Res.* **25,** 2146–2152
7. Schwer, B., and Gross, C. H. (1998) *EMBO J.* **17,** 2086–2094
8. Johnston, L. H., and Thomas, A. P. (1982) *Mol. Gen. Genet.* **186,** 439–444
9. Shea, J. E., Toyn, J. H., and Johnston, L. H. (1994) *Nucleic Acids Res.* **22,** 5555–5564
10. Vaisman, N., Tsouladze, A., Robzyk, K., Ben-Yehuda, S., and Kupiec, M. (1995) *Mol. Gen. Genet.* **247,** 123–136
11. Biggins, S., Bhalla, N., Chang, A., Smith, D. L., and Murray, A. W. (2001) *Genetics* **159,** 453–470
12. Ohi, R., Feoktistova, A., McCann, S., Valentine, V., Look, A. T., Lipsick, J. S., and Gould, K. L. (1998) *Mol. Cell. Biol.* **18,** 4097–4108
13. Zhu, W., Rainville, I. R., Ding, M., Bolus, M., Heintz, N. H., and Pederson, D. S. (2002) *Genetics* **160,** 1319–1333
14. Grey, M., Dusterhoft, A., Henriques, J. A., and Brendel, M. (1996) *Nucleic Acids Res.* **24,** 4009–4014
15. Vijayraghavan, U., Company, M., and Abelson, J. (1989) *Genes Dev.* **3,** 1206–1216
16. Vijayraghavan, U., Parker, R., Tamm, J., Iimura, Y., Rossi, J., Abelson, J., and Guthrie, C. (1986) *EMBO J.* **5,** 1683–1695
17. Moreno, S., Klar, A., and Nurse, P. (1991) *Methods Enzymol.* **194,** 795–823
18. Ansari, A., and Schwer, B. (1995) *EMBO J.* **14,** 4001–4009
19. Derisi, J. L., Iyer, V. R., and Brown, P. O. (1997) *Science* **278,** 680–686
20. Wang, Y., Liu, C. L., Storey, J. D., Tibshirani, R. J., Herschlag, D., and Brown, P. O. (2002) *Proc. Natl. Acad. Sci. U. S. A.* **99,** 5860–5865
21. Urushiyama, S., Tani, T., and Ohshima, Y. (1996) *Mol. Gen. Genet.* **253,** 118–127
22. Eisen, M. B., Spellman, P. T., Brown, P. O., and Botstein, D. (1998) *Proc. Natl. Acad. Sci. U. S. A.* **95,** 14863–14868
23. Kim, S. H., and Lin, R. J. (1996) *Mol. Cell. Biol.* **16,** 6810–6819
24. Clark, T. A., Sugnet, C. W., and Ares, Jr. M. (2002) *Science* **296,** 907–910
25. Jones, M. H., Frank, D. N., and Guthrie, C. (1995) *Proc. Natl. Acad. Sci. U. S. A.* **92,** 9687–9691
26. Chawla, G., Sapra, A. K., Surana, U., and Vijayraghavan, U. (2003) *Nucleic Acids Res.* **31,** 2333–2343
27. Gasch, A. P., Spellman, P. T., Kao, C. M., Carmel-Harel, O., Eisen, M. B., Storz, G., Botstein, D., and Brown, P. O. (2000) *Mol. Biol. Cell* **11,** 4241–4257
28. Ben-Yehuda, S., Dix, I., Russell, C. S., Levy, S., Beggs, J. D., and Kupiec, M. (1998) *RNA* (*N. Y.*) **4,** 1503–1517
29. Lindsey, A.L., and Garcia-Blanco, M.A. (1998) *J. Biol. Chem.* **273,** 32771–32775
30. Lindsey-Boltz, L., Chawla, G., Srivivasan, N., Vijayraghavan, U., and Garcia-Blanco, M.A. (2000) *RNA* (*N. Y.*) **6,** 1289–1305
31. Lee, T. I., Causton, H. C., Holstege, F. C. P., Shen, W. C., Hannett, N., Jennings, E. G., Winston, F., Green, M. R., and Young, R. A. (2000) *Nature* **405,** 701–704
32. Shen, W., Bhaumik, S. R., Causton, H. C., Simon, I., Zhu, X., Jennings, E. G., Wang, T., Young, R. A., and Green, M. R. (2003) *EMBO J.* **22,** 3395–3402
33. Johnson, J. M., Castle, J., Garrett-Engele, P., Kan, Z., Loerch, P. M., Armour, C. D., Santos, R., Schadt, E. E., Stoughton, R., and Schumaker, D. D. (2003) *Science* **302,** 2141–2144
34. Zhu, J., Shendure, J., Mitra, R. D., and Church, G. M. (2003) *Science* **301,** 836–838
35. Dahan, O., and Kupiec, M. (2004) *Nucleic Acids Res.* **32,** 2529–2540
36. Umen, J. G., and Guthrie, C. (1995) *RNA* (*N. Y.*) **1,** 584–597
37. Ben-Yehuda, S., Russell, C. S., Dix, I., Beggs, J. D., and Kupiec, M. (2000) *Genetics* **154,** 61–71
38. McPheeters, D. S., and Muhlenkamp, P. (2002) *Mol. Cell. Biol.* **23,** 4174–4186
39. Thompson-Jager, S., and Domdey, H. (1987) *Mol. Cell. Biol.* **7,** 4010–4016
40. Gavin, A. C., Bosche, M., Krause, R., Grandi, P., Marzioch, M., Bauer, A., Schultz, J., Rick, J. M., Michon, A. M., Cruciat, C. M., Remor, M., Hofert, C., Schelder, M., Brajenovic, M., Ruffner, H., Merino, A., Klein, K., Hudak, M., Dickson, D., Rudi, T., Gnau, V., Bauch, A., Bastuck, S., Huhse, B., Leutwein, C., Heurtier, M. A., Copley, R. R., Edelmann, A., Querfurth, E., Rybin, V., Drewes, G., Raida, M., Bouwmeester, T., Bork, P., Seraphin, B., Kuster, B., Neubauer, G., and Superti-Furga, G. (2002) *Nature* **415,** 141–147
41. Ohi, M. D., Link, A. J., Ren, L., Jennings, J. L., McDonald, W. H., and Gould, K. L. (2002) *Mol. Cell. Biol.* **22,** 2011–2024
42. Ben-Yehuda, S., Dix, I., Russell, C. S., McGarvey, M., Beggs, J. D., and Kupiec, M. (2000) *Genetics* **156,** 1503–1517
43. Chung, S., McLean, M. R., and Rymond, B.C. (1999) *RNA* (*N. Y.*) **5,** 1042–1054

[2] A. K. Sapra and U. Vijayraghavan, unpublished observations.